Liver metastasis models of colon cancer for evaluation of drug efficacy using NOD/Shi-*scid IL2Rγ^{null}* (NOG) mice

KENJI HAMADA[1,2], MAKOTO MONNAI[1,3], KENJI KAWAI[1], CHIYOKO NISHIME[1], CHIKA KITO[1], NORIYUKI MIYAZAKI[4], YASUYUKI OHNISHI[1], MASATO NAKAMURA[1,4,5] and HIROSHI SUEMIZU[1]

[1]Biomedical Research Department, Central Institute for Experimental Animals, 1430 Nogawa, Miyamae, Kawasaki, Kanagawa 216-0001; [2]Pharmaceutical Research Department II, Chugai Pharmaceutical Co., Ltd. and [3]Chugai Research Institute for Medical Science, Inc., 200 Kajiwara, Kamakura, Kanagawa 247-8530; [4]Department of Pathology, Tokai University School of Medicine, Bohseidai, Isehara, Kanagawa 259-1193; [5]Department of Pathology, Tokai University School of Medicine, Hachioji Hospital, 1838 Ishikawa, Hachioji, Tokyo 192-0032, Japan

Received August 17, 2007; Accepted October 1, 2007

Abstract. To examine the drug efficacy of a novel farnesyltransferase inhibitor (FTI), CH4512600, *in vivo*, we developed a reliable liver metastasis model of human colon cancer using NOD/Shi-*scid IL2Rγ^{null}* (NOG) mice. Eleven human colon cancer cell lines were examined for their ability to form diverse metastatic foci in the livers of NOG mice. When inoculated with 10^4 COLO320DM, HCT 116, HT-29, WiDr, LoVo and LS174T cells, liver metastasis was evident in 100% (6/6), 100% (6/6), 88.9% (8/9), 87.5% (7/8), 83.3% (5/6) and 50.0% (3/6) of the NOG mice, respectively. CaCo2, COLO201, LS123, SW48 and SW1417 showed no metastasis when seeded at 10^4 cells even in NOG mice. The mRNA expression levels and genetic mutations of *N, H* and *K-RAS* genes, which directly affect the levels of cellular RAS protein that would be molecular target for FTI, were also examined in these six metastatic human colon cancer cell lines for molecular biological and genotypic characteristics. Only three cell lines had a point mutation in the *RAS* oncogene. LS174T cell line had a point mutation of the *K-RAS* gene at codon 12 (gly12→asp; G12D), and HCT 116 and LoVo cell lines had a point mutation of the *K-RAS* gene at codon 13 (gly13→asp; G13D). Relative gene expression levels of *N, H* and *K-RAS* genes in the HCT 116 cell line were 2.6-5.0-fold lower than that of LS174T and LoVo cell lines. We selected HCT 116 cell line from our liver metastasis model for evaluation of FTI CH4512600 efficacy *in vivo*. Using the NOG mouse liver metastasis model, we demonstrated the effectiveness of FTI CH4512600 to suppress tumor growth *in vivo* and to prolong mouse survival significantly from 36.9±2.9 to 50.3±9.4 days.

Correspondence to: Dr Hiroshi Suemizu, Central Institute for Experimental Animals, 1430 Nogawa, Miyamae, Kawasaki, Kanagawa 216-0001, Japan
E-mail: suemizu@ciea.or.jp

Key words: NOD/Shi-*scid IL2Rγ^{null}* mice, NOG mice, liver metastasis model, human colon cancer, farnesyltransferase inhibitor

Introduction

Colon cancer is one of the major cancers (1,2). Despite resection of colorectal cancer, about half of the patients suffer recurrence from metastasis. The liver is the major site of metastasis of colon cancer (3-6); but only limited numbers of patients who suffer metastasis are candidates for surgery. The alternative method to treat liver metastasis is chemotherapy; therefore, establishment of a liver metastasis model effective for evaluating compounds is important.

RAS is a guanine nucleotide binding GTPase that transduces developmental and proliferative information from extracellular signals to the nucleus (7,8). In normal cells, activation of RAS is mediated by nucleotide exchange factors that catalyze the exchange of GDP (inactive form) with GTP (active form), whereas its inactivation is mediated by GTPase-activating proteins (7). A large number of human cancers (30%) harbor mutations in the RAS protein that result in GTP-locked RAS, which is constitutively activated and is believed to contribute to uncontrolled malignant growth (9). Therefore, blocking the reckless RAS signal is an attractive target for chemotherapy. RAS requires a lipid post-translational modification (farnesylation) for its cancer-causing activity (10,11). The modification is catalyzed by FTase, which attaches farnesyl to the cysteine of the RAS carboxyl-terminal tetrapeptide CAAX (12-16). Because farnesylation of RAS is required and sufficient for its transforming activity (17,18), an intense search for FTase inhibitors (FTIs) with potential anticancer activity is under way (10,11). Many FTIs are reported to have potent tumor growth inhibitory activity, although their anti-tumor effect is caused not only by blocking of the RAS signaling pathway (19-24).

New strategies for treating metastatic colon cancer will also require the development of appropriate animal models for

studying their effectiveness. NOD/Shi-*scid IL2Rγ*^{null} (NOG) mice have been used for many *in vivo* models with engrafted human cells and tissues, such as human hematopoietic stem cells (25,26), myeloma cells (27,28) and endometrial tissue (29). Moreover, when compared with NOD/Shi-*scid* mice, NOG mice were a superior xenotransplantation system for the engraftment of human cancer cells (30). Recently, we developed a reliable new model system for assaying hematogenous liver metastasis of pancreatic cancer using NOG mice (31). The liver metastasis incidence and grade of each of the pancreatic cancer cell lines were quantitatively evaluated, and were dose-dependent over a wide range of inoculation doses.

In this study, we first examined the *in vivo* biological behavior of eleven human colon cancer cell lines using the NOG mouse liver metastasis model. Then, we examined human colon cancer cell lines that possessed liver metastatic potentials in terms of the molecular biological behavior of the target molecules. In this case, *RAS* oncogene mutation and gene expression are molecular targets for the FTI. We selected the HCT 116 cell line from our liver metastasis panel for evaluation of FTI CH4512600 efficacy *in vivo* and demonstrated its effectiveness through significantly prolonged mouse survival. This liver metastasis model using NOG mice should respond flexibly in efficacy evaluations of all types of anti-cancer drugs.

Materials and methods

Cells. CaCo2, COLO201, COLO320DM, HCT 116, HT-29, LoVo, LS123, LS174T, SW48, SW1417 and WiDr were obtained from the American Type Culture Collection (Manassas, VA). COLO201 and COLO320DM were maintained in RPMI1640 (Sigma, St. Louis, MO) supplemented with 10% fetal bovine serum (FBS, Hyclone, UT). HCT 116 and HT-29 were maintained in McCoy's 5A (Sigma), LoVo was maintained in Ham's F12K (Sigma), SW48 and SW1417 were maintained in Leibovitz's L-15 (Sigma), and LS123, LS174T and WiDr were maintained in Dulbecco's modified Eagle's medium (DMEM, Sigma). All culture medium were supplemented with antibiotics and 10% FBS, except for the CaCo2 cell line. DMEM containing 20% was used for CaCo2. Cells were incubated in a humidified (37˚C, 5% CO_2) incubator and passaged on reaching 80% confluence. SW48 and SW1417 were incubated in a 100% air (37˚C) incubator and passaged on reaching 80% confluence.

Liver metastasis assay. This study was performed in accordance with the institutional guidelines and was approved by the Animal Experimentation Committee of the Central Institute for Experimental Animals. We bred NOD/Shi-*scid IL2Rγ*^{null} (NOG) mice, and used them at the age of 7-9 weeks. Sub-confluent culture of colon cancer cells was harvested with trypsin-EDTA solution. Collected cells were washed and suspended in serum-free medium at a concentration of $2x10^5$ cells per ml. Experimental liver metastases were generated by intrasplenic injection of 10^4 of cancer cells (50 μl of cell suspension) and splenectomy (9). The mice were sacrificed 6 weeks later, and liver metastases were enumerated immediately, without fixation.

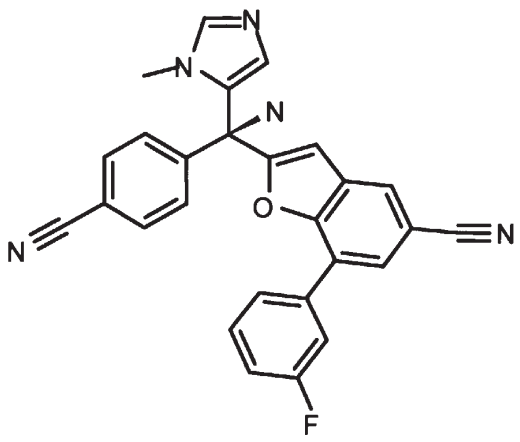

Figure 1. Chemical structure of FTI CH4512600.

RAS oncogene mutation and gene expression analyses. Total cellular RNA was obtained from 90% confluent cultures of colon cancer cell lines using the RNeasy Mini kit (Qiagen K.K. Tokyo, Japan). The reverse transcription polymerase chain reaction (RT-PCR) was performed using the GeneAmp RNA PCR Kit (Applera Corp., Applied Biosystems, CA). *N*, *H* and *K-RAS* oncogene mutations were analyzed by the PCR-direct sequencing method with the following primer sets, H-Nras-F: TGTGGTCCTAAATCTGTCCAAAGC and H-Nras-R: GTCAGTGCAGCTTGAAAGTGGC, H-Hras-F: GTGAACGGTGGGGCAGGAGACC and H-Hras-R2: CTG CATCCGGCACCTCCATGT, and H-Kras-F: CGGGAGAG AGGCCTGCTGAA and H-Kras-R: AAATTACCACTTGT ACTAGTATGCCTT, respectively. For quantitative analysis, an aliquot of cDNA was added to the Master Mix of SYBR *Premix Ex Taq*™ (Perfect Real Time, Takara Bio Inc., Shiga, Japan), and quantitative gene expression data were acquired using an ABI PRISM 7700 Sequence Detection System (Applera Corp., Applied Biosystems). PCR primers for detecting each *RAS* oncogene were obtained from Takara Bio Inc. RT-PCR of GAPDH RNA was used to standardize results.

Gene expression analysis for angiogenesis-related VEGF isoforms. Novel FTI compound, CH4512600 (see structure in Fig. 1) was added to sub-confluent HCT 116 cultures at concentrations of 1 and 10 μM, and further incubated for 24 h. Total cellular RNA isolation was as described above. Quantitative analyses for VEGF-A and VEGF-A isoform (VEGF121, VEGF165, and VEGF189) gene expression were performed using TaqMan Universal PCR Master Mix (PE Applied Biosystems, Foster City, CA, USA) according to the manufacturer's instructions. The primers used in this study were as follows: VEGF-A-F: CTTGCCTTGCTGCTCTACCT, VEGF-A-R: GATTCTGCCCTCCTCCTTCTG, VEGF-A-probe: CATGCCAAGTGGTCCC, VEGF189-F: GCGGAA ATCCCGGTATAAGT, VEGF189-R: GCTTTCTCCGCTC TGAGCAA, VEGF189-probe: CCTGGAGCGTTCCCTG, VEGF165-F: ACAACAAATGTGAATGCAGACCAA A, VEGF165-R: GCTTTCTCCGCTCTGAGCAA, VEGF165-probe: CCACAGGGATTTTCT, VEGF121-F: ACAACAAA TGTGAATGCAGACCAAA, VEGF121-R: CTGAGGGAG

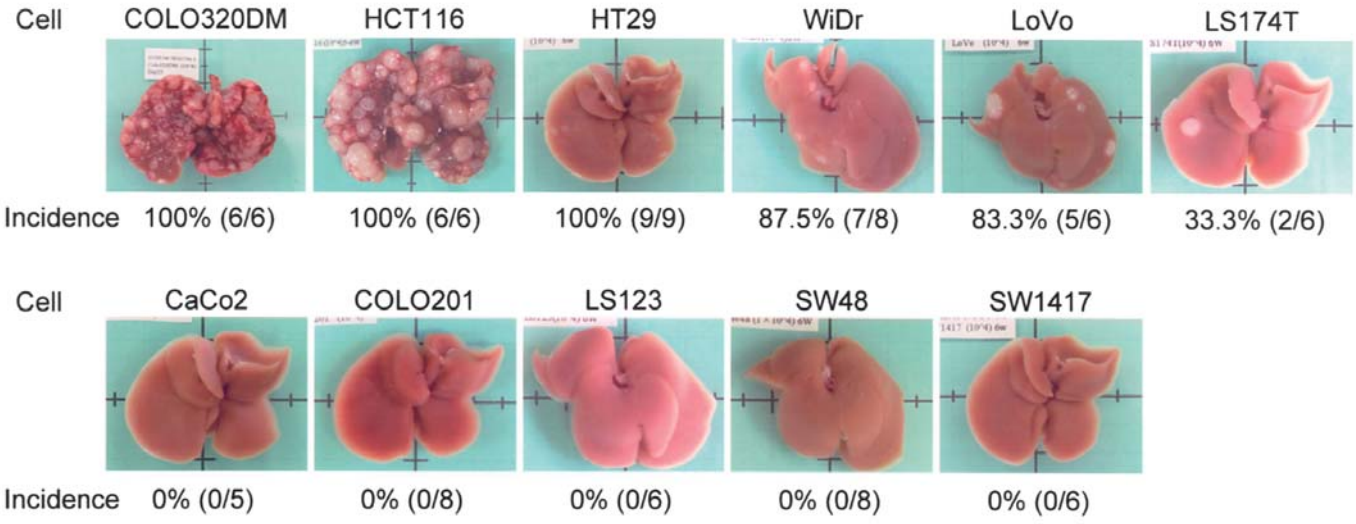

Figure 2. Representative gross findings of liver metastases of human colon cancer cell lines. Eleven human colon cancer cell lines: CaCo2, COLO201, COLO320DM, HCT 116, HT-29, LoVo, LS123, LS174T, SW48, SW1417 and WiDr, were intrasplenically implanted into NOG mice. The mice were sacrificed 6 weeks later, and liver metastases were enumerated immediately, without prior fixation.

GCTCCTTCCT, VEGF121-probe: CAAGAAAAATGTGA CAAGCCG, and for the internal control, ß-actin-probe-primer mix (PE Applied Biosystems). Quantitative gene expression data were acquired using an ABI PRISM 7000 Sequence Detection System (Applera Corp., Applied Biosystems).

Immunohistochemical staining. Sections (4-μm-thick) were cut from formalin-fixed and paraffin-embedded tissue blocks. Immunohistochemical staining was performed using the streptavidin-biotin method. An affinity-purified rabbit polyclonal anti-VEGF antibody (A-20, Santa Cruz) at 1:100 dilution was used. After 30 min of incubation at room temperature, sections were incubated with peroxidase-labeled anti-rabbit Ig antibody, Histofine Simple Stain MAX PO (Nichirei Bioscience, Japan), for another 30 min at room temperature. Peroxidase activity was detected with diaminobenzidine (Dojin, Japan). Sections were counter-stained with hematoxylin and dehydrated.

Drug efficacy studies of CH4512600 in a NOG mouse liver metastasis model. Thirty-two NOG mice were intrasplenically injected with 10^4 HCT 116 cells. After three days, the mice were randomized and divided into 4 groups in order to start administration. Control animals received a saline vehicle. FTI CH4512600 was administered daily for three weeks via peroral administration (50 and 250 mg/kg). Type I DNA topoisomerase inhibitor, CPT-11, was administered weekly for three weeks via intravenous injection as positive control.

Statistical analysis. The Kaplan-Meier log-rank method was used with SAS preclinical package software ver. 5.0.

Results

Selection of a suitable cell line for evaluating the FTI drug efficacy from the panel of liver metastasis models. To examine novel FTI CH4512600 (Fig. 1) efficacy in liver metastasis, we established a liver metastasis model of human colon cancer using NOD/Shi-s*scid IL2R*γ^{null} (NOG) mice. Liver metastasis capability was first examined at autopsy within 6 weeks after 10^4 cells were transplanted intrasplenically. Eleven human colon cancer cell lines (COLO320DM, HCT 116, HT-29, WiDr, LoVo, LS174T, SW1417, SW48, LS123, COLO201 and CaCo2) formed diverse metastatic foci in the liver of the NOG mice (Fig. 2). CaCo2, COLO201, LS123, SW48 and SW1417 showed no metastasis with 10^4 cells. On the other hand, COLO320DM and HCT 116 metastasized in 100% (6/6) of the mice. HT-29, WiDr, LoVo and LS174T metastasized in 88.9% (8/9), 87.5% (7/8), 83.3% (5/6) and 50.0% (3/6) of the mice, respectively. The minimum requirement for the cells to be a target cell for FTI efficacy testing is a high liver metastasis potency in the NOG mice model. Six out of eleven cell lines, which were able to metastasize to the liver in the NOG mouse model, cleared the minimum requirement for this FTI target. These six cell lines were examined for mRNA expression and genetic mutations of *N, H* and *K-RAS* genes, which directly affect the levels of cellular RAS protein as a molecular target for FTI CH4512600. Comparison of the *RAS* oncogene mutation and relative gene expression among six colon cancer cell lines is shown in Table I. No *N-RAS* mutations were observed in six colon cancer cell lines we used. Nucleotide sequences of *H-RAS* gene in COLO320DM, HCT 116, HT-29 and WiDr showed some differences from the reported sequence, but the differences did not involve any changes in their amino acid sequences (silent mutation). In the *K-RAS* oncogene, COLO320DM showed a silent mutation at codon 173 (GAT→GAC), LS174T had a point mutation at codon 12 (G12D; GGT→GAT), and HCT 116 and LoVo had a point mutation of the *K-RAS* gene at codon 13 (G13D; GGC→GAC). Compared with the *N, H* and *K-RAS* gene expression levels that were standardized with GAPDH expression among the six cell lines, the HCT 116

Table I. Comparison of *RAS* oncogene mutations and relative gene expression among six colon cancer cell lines.

Cell line	*N-RAS*		*H-RAS*		*K-RAS*	
	Point mutation	Gene expression[a]	Point mutation	Gene expression[a]	Point mutation	Gene expression[a]
COLO320DM	-	2.5	Lys 5, silent (AAG→AAA)	1.0	Asp 173, silent (GAT→GAC)	1.6
HCT116	-	1.0	His 27, silent (CAT→CAC)	1.0	Gly 13→Asp (GGC→GAC)	1.0
HT29	-	2.3	His 27, silent (CAT→CAC)	2.7	-	1.8
WiDr	-	2.3	Gly 15, silent (GGG→GGC) His 27, silent (CAT→CAC)	4.5	-	3.3
LoVo	-	4.0	-	2.9	Gly 13→Asp (GGC→GAC)	5.0
LS174T	-	4.3	-	2.6	Gly 12→Asp (GGT→GAT)	2.6

[a]All *RAS* gene (*N, H* and *K*) expressions are normalized to the each *RAS* gene expression level in HCT 116, which were given a value of 1.0 in each experiment.

cell line showed the lowest expression level among all *RAS* oncogenes. The *RAS* gene (*N, H* and *K*) expressions were normalized to each of the *RAS* gene expression levels in HCT 116, which were given a value of 1.0 in each experiment. Relative gene expression levels of *N, H* and *K-RAS* genes in the HCT 116 cell line were 2.6-5.0-fold lower than that of the LS174T and LoVo cell lines.

Drug efficacy studies of FTI CH4512600 in the NOG mice liver metastasis model. We selected the HCT 116 cell line from our panel of liver metastasis models using NOG mice for evaluating FTI CH4512600 efficacy *in vivo*. HCT 116 cells (10^4) were injected intrasplenically into the NOG mouse liver; the degree of liver metastasis was monitored periodically. Doses of 50 and 250 mg/kg of FTI CH4512600 were administered daily for 3 weeks starting from 3 days after the injection of HCT 116 cells. At day 28 (25 days after the start of administration), administration of 50 mg/kg FTI CH4512600 slightly suppressed, and 250 mg/kg FTI CH4512600 discernibly suppressed the transplanted HCT 116 cell growth in the liver metastasis model. Furthermore, administration of 250 mg/kg FTI CH4512600 dramatically suppressed HCT 116 tumor growth in this model at day 35 (32 days after the start of administration) (Fig. 2). However, low-dose (50 mg/kg) administration was not sufficient to inhibit tumor growth completely.

Vascular endothelial growth factor (VEGF)-dependent angiogenesis was thought to be affected by *RAS* oncogene status, which is the molecular target for FTIs. We examined VEGF expression in our FTI efficacy-testing model. Immunohistochemical staining with anti-VEGF antibody was performed in HCT 116 colon cancer cell metastasized NOG liver. In a non-FTI CH4512600-treated liver metastatic focus at day 35, VEGF-expressing cells were observed to have a strong reaction product for immunoperoxidase staining (Fig. 4b). On the other hand, at day 35 when the most effective drug efficacy at 250 mg/kg FTI CH4512600 appeared, no VEGF-expressing cells, which showed a strong positive reaction in the non-treated group, were observed. Only a few, weakly VEGF-expressing cells were observed. To confirm the effect of FTI CH4512600 on VEGF expression, mRNA levels of VEGF isoform were compared between non-treated and FTI CH4512600-treated HCT 116 cells *in vitro*. After 24 h, relative mRNA levels of VEGF121, VEGF165, and VEGF189 were reduced dose-dependently by addition of FTI CH4512600 (Fig. 5). Addition of FTI CH4512600 to culture medium of HCT 116 cells also resulted in suppression of VEGF expression *in vitro*.

We described the effectiveness of FTI CH4512600 in complete suppression of HCT 116 cell growth in the NOG mouse liver metastasis model. Finally, we confirmed the systemic anti-cancer effects of FTI CH4512600; a survival study was carried out with or without administration of drugs in the NOG mouse liver metastasis model. Thirty-two mice were intrasplenically injected with 10^4 HCT 116 cells and 3 days later, they were divided into 4 groups (n=8) for a survival study. Type I DNA topoisomerase inhibitor CPT-11 was used as a positive control. As shown in Fig. 6a, neither FTI CH4512600 nor CPT-11 treatment had any effect on body weight change throughout the experiment. Unfortunately, 2 of 8 CPT-11-treated mice died from the toxicity of the compound immediately after administration; these two mice

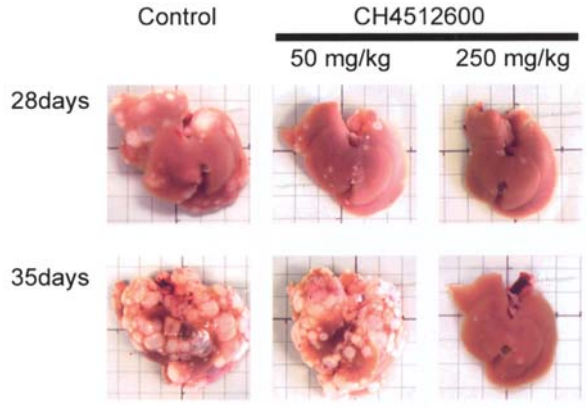

Figure 3. Effects of FTI CH4512600 on the liver metastasis model. HCT 116 cells (10^4 cells) transplanted into mouse liver was dissected at day 28 and day 35. FTI CH4512600 (50 and 250 mg/kg, daily) was administered for 3 weeks (as described in Materials and methods). Representative results are shown here (n=3).

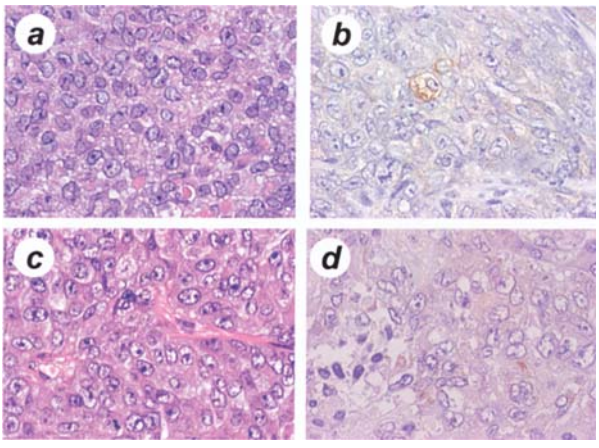

Figure 4. Immunohistochemical staining for VEGF protein in liver metastatic focus in NOG mice. Hematoxylin-eosin staining of the liver metastatic focus of non-treated control (a) and FTI CH4512600-treated mice (c). Immunohistochemical staining with anti-VEGF antibody of the liver metastatic focus of non-treated (b) and FTI CH4512600-treated mice (d).

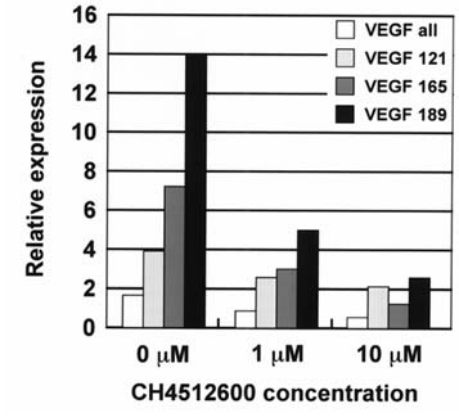

Figure 5. Quantitative RT-PCR HCT 116 cells were cultured in the presence or absence of FTI CH4512600 for 24 h. Total cellular RNA was isolated and reverse-transcripted to cDNA for quantitative RT-PCR. Relative mRNA expression levels of VEGF121, 165, 189 and total VEGF normalized by ß-actin are shown.

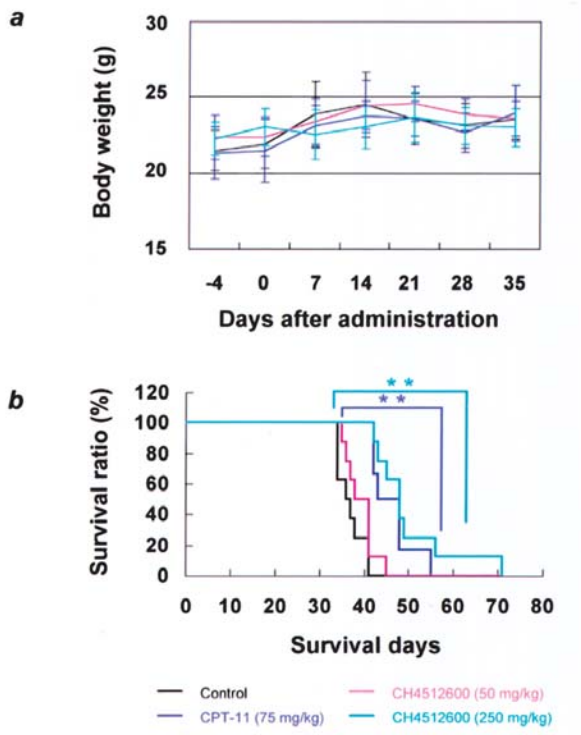

Figure 6. Body weight change (a) and survival rate (b) of HCT 116-transplanted mice for vehicle control (n=8), CH4512600 (n=8) and CPT-11-treated mice (n=6). Administration was started 3 days after the inoculation (day 0). Black line, vehicle control; blue line, CPT-11 (75 mg/kg); red line, CH4512600 (50 mg/kg); light blue line, CH4512600 (250 mg/kg). Statistical significance between control and 250 mg/kg of CH4512600 ($P<0.0001$) and control and 75 mg/kg of CPT-11 ($P=0.0003$) was calculated using SAS preclinical package ver.5.0.

were excluded from the statistical analysis. Untreated mice died within 44 days after HCT 116 injection (range 34-41 days after treatment initiation, mean ± SD: 36.9±2.9 days), which was statistically no different than the mean survival for 50 mg/kg FTI CH4512600-treated mice (39.3±3.3 days). These data corresponded to the degree of metastasis in mice treated with 50 mg/kg FTI CH4512600 on day 35 as shown in Fig. 2. On the other hand, treatment with 250 mg/kg of FTI CH4512600 (50.3±9.4, $P<0.0001$) and 75 mg/kg CPT-11 (46.3±5.1, $P=0.0003$) significantly prolonged mouse survival compare with that of vehicle control (Fig. 6b).

Discussion

The human xenograft model with cancer cells implanted in subcutaneous spaces of athymic nude mice or severe combined immunodeficiency (*scid*) mice has been the mainstream for evaluating drug efficacy *in vivo*. When a novel FTI compound was developed, efficacy studies were first performed using the xenograft model. Kohl *et al* (32) first reported the effectiveness of FTI L-739,749 on *Ras*-dependent tumor growth in nude mice. Thereafter, various FTIs such as FTI-276, LB42722 and SCH66336 were developed and their efficacies were evaluated in the xenograft model (33-35). We are interested not so much in suppression of primary tumor growth as in suppression of metastatic tumor growth *in situ*, particularly liver metastasis of colorectal tumors. However, the previous

models only evaluated *in vivo* cell growth. Recently, we developed a reliable and quantitative liver metastasis model using NOG mice (31). With this model, we observed differential *in vivo* growth characteristics between the subcutaneous space and liver. Human pancreatic cancer cell lines, BxPC-3 and Capan-2, grew well in the subcutaneous space but when injected intrasplenically, these cells were scarcely able to grow in the liver. Therefore, we had to first select a suitable colon cancer cell line, which can metastasize and grow well after intrasplenic injection, to be the FTI target. In this study, we developed a reliable liver metastasis model for colon cancer using NOG mice as an *in vivo* FTI efficacy evaluation model. This liver metastasis model using NOG mice more closely mimics the *in vivo* conditions in patients with colon cancer. Another *in vivo* FTI efficacy evaluation model was reported by Lantry *et al* (36). They used a lung adenoma chemically induced in A/J mice by 4-(methylnitrosamino)-1-(3-pyridyl)-1-butanone (NNK) administration as the FTI target, and demonstrated FTI efficacy in a primary tumor model. In addition, the reduction in total tumor volume with treatment is the first demonstration of inhibition of tumor development by FTI in a murine primary lung tumor model.

Antitumor efficacy of FTI-276 was evaluated in a nude mouse xenograft model using two human lung carcinoma cell lines: one (Calu-1) with a *K-RAS* oncogenic mutation and the other (NCI-H810) with no *RAS* mutations (33). The Calu-1 tumors from control animals (treated with saline once daily for 36 days) grew to an average size of 556±59 mm^3. In contrast, tumors treated once daily with FTI-276 (50 mg/kg) grew very little, and the average tumor size was 113±44 mm^3. Thus, FTI-276 essentially blocked tumor growth of Calu-1 carcinoma, with no evidence of gross toxicity. In contrast to Calu-1, NCI-H810 carcinomas were not sensitive to FTI-276 treatment. These results suggested that FTI-276 inhibition of growth of human lung carcinomas was RAS dependent. The specificity of FTI L-739,749 was also evaluated for inhibition of RAS-dependent tumor growth in Ratl cells transformed with either oncogenically mutated human *N, H*, or *K-Ras* oncogenes (32). In addition to genetic mutation of *RAS* oncogenes, FTI efficacy should be affected by the levels of RAS protein, especially in the active form, or the levels of RNA expression of *RAS* oncogenes. High-grade astrocytomas do not harbor oncogenic/activating *RAS* mutations (37-39); however, RAS activation does occur in these tumors, attributable in part to overexpression of receptor tyrosine kinases (39). Two of the three human glioblastoma multiforme (GBM) xenografts showed substantial growth inhibition in response to FTI SCH66336, with ≤69% growth inhibition after 21 days of treatment (35). These data indicated that the absence of *RAS* mutations did not preclude chemotherapeutic efficacy by FTIs, with RAS likely to be a major target of FTIs regardless of *RAS* mutational status. Therefore, we checked the *RAS* mutational status and their expression levels in colon cancer cell lines, which showed metastatic ability in the NOG mouse model prior to selection of the FTI target cell line. Since *K-RAS* mutations are very common in human cancers, we selected the HCT 116 human colon cancer cell line that has a *K-RAS* mutation (G13D) as a target cells for FTI efficacy study. In our metastasis model, treatment with 250 mg/kg of FTI CH4512600 strongly suppressed transplanted HCT 116 cancer cell growth in the liver and showed statistically significant prolongation of mouse survival without any toxicity.

The process of tumor metastasis can be divided to several steps: initially tumor cells separate from the original tumor mass and invade a blood vessel; then they are carried in the bloodstream, and finally adhere to the site of metastasis and proliferate (40). Our liver metastasis model mimics only the latter part of metastasis. Angiogenic factor VEGF is thought to be one of the important factors for developing liver metastasis (40). Oncogenic RAS is known to upregulate expression of VEGF, acting via either the Raf/MAPK or the PI3K pathway (41,42). In contrast, FTI led to a down-regulation of *VEGF* mRNA in *RAS*-transformed cells (34). Furthermore, L-744,832 potently inhibits the secretion of VEGF by these cells and, hence, may also demonstrate an antiangiogenic effect *in vivo* (43). Our *in vitro* experiment also demonstrated that HCT 116 human colon cancer cells down-regulated VEGF gene expression by addition of FTI CH4512600. Feldkamp *et al* reported that viable regions of vehicle-treated human glioblastoma multiforme (GBM) showed robust VEGF expression; in contrast, few components of drug-treated FTI SCH66336-treated GBM were viable, with a disorganized histological architecture, and weak VEGF expression (35). Immunohistochemical staining with anti-VEGF antibody in NOG mouse liver, after intrasplenic injection with HCT 116 cells revealed that administration of 250 mg/kg FTI CH4512600 induced not only a decrease in the positive cell number but also weakened the positive signals. These results suggested that angiogenic factor VEGF is partially involved in developing liver metastasis.

In conclusion, we demonstrated that treatment with novel FTI CH4512600 strongly suppressed transplanted HCT 116 cancer cell growth in the liver of NOG mice used as a liver metastasis model and significantly prolonged survival without any toxicity. Our liver metastasis model developed using NOG mice is reliable and more closely mimics *in vivo* conditions in patients with colon cancer compared with the traditional xenograft model created by cancer cell transplantation into a subcutaneous space. Our panel of eleven colon cancer cell lines for liver metastasis is applicable to evaluation of the safety, efficacy, and medicinal benefits of new anticancer drugs.

Acknowledgments

We thank Chie Yagihashi and Noriko Omi (CIEA) for their excellent technical assistance.

References

1. Jemal A, Murray T, Ward E, Samuels A, Tiwari RC, Ghafoor A, Feuer EJ and Thun MJ: Cancer statistics, 2005. CA Cancer J Clin 55: 10-30, 2005.
2. Boyle P and Ferlay J: Cancer incidence and mortality in Europe, 2004. Ann Oncol 16: 481-488, 2005.
3. Ballantyne GH and Quin J: Surgical treatment of liver metastases in patients with colorectal cancer. Cancer 71: 4252-4266, 1993.
4. Cromheecke M, De Jong KP and Hoekstra HJ: Current treatment for colorectal cancer metastatic to the liver. Eur J Surg Oncol 25: 451-463, 1999.

5. Biasco G and Gallerani E: Treatment of liver metastases from colorectal cancer: what is the best approach today? Dig Liver Dis 33: 438-444, 2001.
6. Ruers T and Bleichrodt RP: Treatment of liver metastases, an update on the possibilities and results. Eur J Cancer 38: 1023-1033, 2002.
7. McCormick F: Signal transduction. How receptors turn Ras on. Nature 363: 15-16, 1993.
8. McCormick F: Activators and effectors of ras p21 proteins. Curr Opin Genet Dev 4: 71-76, 1994.
9. Barbacid M: Important Advances in Oncology. J.B. Lippincott, Philadelphia, pp3-22, 1986.
10. Gibbs JB: Ras C-terminal processing enzymes - new drug targets? Cell 65: 1-4, 1991.
11. Pendergast AM, Quilliam LA, Cripe LD, Bassing CH, Dai Z, Li N, Batzer A, Rabun KM, Der CJ and Schlessinger J: BCR-ABL-induced oncogenesis is mediated by direct interaction with the SH2 domain of the GRB-2 adaptor protein. Cell 75: 175-185, 1993.
12. Hancock JF, Magee AI, Childs JE and Marshall CJ: All ras proteins are polyisoprenylated but only some are palmitoylated. Cell 57: 1167-1177, 1989.
13. Casey PJ, Solski PA, Der CJ and Buss JE: p21ras is modified by a farnesyl isoprenoid. Proc Natl Acad Sci USA 86: 8323-8327, 1989.
14. Reiss Y, Goldstein JL, Seabra MC, Casey PJ and Brown MS: Inhibition of purified p21ras farnesyl:protein transferase by Cys-AAX tetrapeptides. Cell 62: 81-88, 1990.
15. Manne V, Roberts D, Tobin A, O'Rourke E, De Virgilio M, Meyers C, Ahmed N, Kurz B, Resh M and Kung HF: Identification and preliminary characterization of protein-cysteine farnesyltransferase. Proc Natl Acad Sci USA 87: 7541-7545, 1990.
16. Moores SL, Schaber MD, Mosser SD, Rands E, O'Hara MB, Garsky VM, Marshall MS, Pompliano DL and Gibbs JB: Sequence dependence of protein isoprenylation. J Biol Chem 266: 14603-14610, 1991.
17. Jackson JH, Cochrane CG, Bourne JR, Solski PA, Buss JE and Der CJ: Farnesol modification of Kirsten-ras exon 4B protein is essential for transformation. Proc Natl Acad Sci USA 87: 3042-3046, 1990.
18. Kato K, Cox AD, Hisaka MM, Graham SM, Buss JE and Der CJ: Isoprenoid addition to Ras protein is the critical modification for its membrane association and transforming activity. Proc Natl Acad Sci USA 89: 6403-6407, 1992.
19. Venkatasubbarao K, Choudary A and Freeman JW: Farnesyl transferase inhibitor (R115777)-induced inhibition of STAT3(Tyr705) phosphorylation in human pancreatic cancer cell lines require extracellular signal-regulated kinases. Cancer Res 65: 2861-2871, 2005.
20. Beaupre DM, McCafferty-Grad J, Bahlis NJ, Boise LH and Lichtenheld MG: Farnesyl transferase inhibitors enhance death receptor signals and induce apoptosis in multiple myeloma cells. Leuk Lymphoma 44: 2123-2134, 2003.
21. Ferguson D, Rodriguez LE, Palma JP, Refici M, Jarvis K, O'Connor J, Sullivan GM, Frost D, Marsh K, Bauch J, Zhang H, Lin NH, Rosenberg S, Sham HL and Joseph IB: Antitumor activity of orally bioavailable farnesyltransferase inhibitor, ABT-100, is mediated by antiproliferative, proapoptotic, and antiangiogenic effects in xenograft models. Clin Cancer Res 11: 3045-3054, 2005.
22. Head J and Johnston SR: New targets for therapy in breast cancer: farnesyltransferase inhibitors. Breast Cancer Res 6: 262-268, 2004.
23. Alcock RA, Dey S, Chendil D, Inayat MS, Mohiuddin M, Hartman G, Chatfield LK, Gallicchio VS and Ahmed MM: Farnesyltransferase inhibitor (L-744,832) restores TGF-beta type II receptor expression and enhances radiation sensitivity in K-ras mutant pancreatic cancer cell line MIA PaCa-2. Oncogene 21: 7883-7890, 2002.
24. Head JE and Johnston SR: Protein farnesyltransferase inhibitors. Expert Opin Emerg Drugs 8: 163-178, 2003.
25. Ito M, Hiramatsu H, Kobayashi K, Suzue K, Kawahata M, Hioki K, Ueyama Y, Koyanagi Y, Sugamura K, Tsuji K, Heike T and Nakahata T: NOD/SCID/gamma(c)(null) mouse: an excellent recipient mouse model for engraftment of human cells. Blood 100: 3175-3182, 2002.
26. Yahata T, Ando K, Nakamura Y, Ueyama Y, Shimamura K, Tamaoki N, Kato S and Hotta T: Functional human T lymphocyte development from cord blood CD34$^+$ cells in nonobese diabetic/Shi-scid, IL-2 receptor gamma null mice. J Immunol 169: 204-209, 2002.
27. Miyakawa Y, Ohnishi Y, Tomisawa M, Monnai M, Kohmura K, Ueyama Y, Ito M, Ikeda Y, Kizaki M and Nakamura M: Establishment of a new model of human multiple myeloma using NOD/SCID/gammac(null) (NOG) mice. Biochem Biophys Res Commun 313: 258-262, 2004.
28. Dewan MZ, Watanabe M, Terashima K, Aoki M, Sata T, Honda M, Ito M, Yamaoka S, Watanabe T, Horie R and Yamamoto N: Prompt tumor formation and maintenance of constitutive NF-kappaB activity of multiple myeloma cells in NOD/SCID/gammacnull mice. Cancer Sci 95: 564-568, 2004.
29. Matsuura-Sawada R, Murakami T, Ozawa Y, Nabeshima H, Akahira J, Sato Y, Koyanagi Y, Ito M, Terada Y and Okamura K: Reproduction of menstrual changes in transplanted human endometrial tissue in immunodeficient mice. Hum Reprod 20: 1477-1484, 2005.
30. Ikoma N, Yamazaki H, Abe Y, Oida Y, Ohnishi Y, Suemizu H, Matsumoto H, Matsuyama T, Ohta Y, Ozawa A, Ueyama Y and Nakamura M: S100A4 expression with reduced E-cadherin expression predicts distant metastasis of human malignant melanoma cell lines in the NOD/SCID/gammaCnull (NOG) mouse model. Oncol Rep 14: 633-637, 2005.
31. Suemizu H, Monnai M, Ohnishi Y, Ito M, Tamaoki N and Nakamura M: Identification of a key molecular regulator of liver metastasis in human pancreatic carcinoma using a novel quantitative model of metastasis in NOD/SCID/γ_c^{null} (NOG) mice. Int J Oncol 31: 741-751, 2007.
32. Kohl NE, Wilson FR, Mosser SD, Giuliani E, De Solms SJ, Conner MW, Anthony NJ, Holtz WJ, Gomez RP and Lee TJ: Protein farnesyltransferase inhibitors block the growth of ras-dependent tumors in nude mice. Proc Natl Acad Sci USA 91: 9141-9145, 1994.
33. Sun J, Qian Y, Hamilton AD and Sebti SM: Ras CAAX peptidomimetic FTI 276 selectively blocks tumor growth in nude mice of a human lung carcinoma with K-Ras mutation and p53 deletion. Cancer Res 55: 4243-4247, 1995.
34. Zhang B, Prendergast GC and Fenton RG: Farnesyltransferase inhibitors reverse Ras-mediated inhibition of Fas gene expression. Cancer Res 62: 450-458, 2002.
35. Feldkamp MM, Lau N, Roncari L and Guha A: Isotype-specific Ras.GTP-levels predict the efficacy of farnesyl transferase inhibitors against human astrocytomas regardless of Ras mutational status. Cancer Res 61: 4425-4431, 2001.
36. Lantry LE, Zhang Z, Yao R, Crist KA, Wang Y, Ohkanda J, Hamilton AD, Sebti SM, Lubet RA and You M: Effect of farnesyltransferase inhibitor FTI-276 on established lung adenomas from A/J mice induced by 4-(methylnitrosamino)-1-(3-pyridyl)-1-butanone. Carcinogenesis 21: 113-116, 2000.
37. Kiaris H and Spandidos DA: Mutations of *ras* genes in human tumours (review). Int J Oncol 7: 413-421, 1995.
38. Tuzi NL, Venter DJ, Kumar S, Staddon SL, Lemoine NR and Gullick WJ: Expression of growth factor receptors in human brain tumours. Br J Cancer 63: 227-233, 1991.
39. Guha A, Feldkamp MM, Lau N, Boss G and Pawson A: Proliferation of human malignant astrocytomas is dependent on Ras activation. Oncogene 15: 2755-2765, 1997.
40. Takeda A, Stoeltzing O, Ahmad SA, Reinmuth N, Liu W, Parikh A, Fan F, Akagi M and Ellis LM: Role of angiogenesis in the development and growth of liver metastasis. Ann Surg Oncol 9: 610-616, 2002.
41. Chen C, Pore N, Behrooz A, Ismail-Beigi F and Maity A: Regulation of glut1 mRNA by hypoxia-inducible factor-1. Interaction between H-ras and hypoxia. J Biol Chem 276: 9519-9525, 2001.
42. Berra E, Pagès G and Pouysségur J: MAP kinases and hypoxia in the control of VEGF expression. Cancer Metastasis Rev 19: 139-145, 2000.
43. Rak J, Mitsuhashi Y, Bayko L, Filmus J, Shirasawa S, Sasazuki T and Kerbel RS: Mutant ras oncogenes upregulate VEGF/VPF expression: implications for induction and inhibition of tumor angiogenesis. Cancer Res 55: 4575-4580, 1995.